Available online at www.sciencedirect.com
ScienceDirect
Acta Materialia 55 (2007) 6705–6712
Acta MATERIALIA
www.elsevier.com/locate/actamat

Microstructure near corners of continuous-cast steel slabs showing three-dimensional frozen meniscus and hooks

Go-Gi Lee [a], Brian G. Thomas [b,*], Seon-Hyo Kim [a], Ho-Jung Shin [c], Seung-Kwan Baek [d], Choon-Haeng Choi [d], Dong-Su Kim [d], Sung-Jong Yu [d]

[a] *Department of Materials Science and Engineering, Pohang University of Science and Technology, South Korea*
[b] *Department of Mechanical Science and Engineering, University of Illinois at Urbana-Champaign, IL, USA*
[c] *POSCO Technical Research Laboratories, Continuous Casting, POSCO, Gwangyang Works, South Korea*
[d] *POSCO Steelmaking Department, Technology Development Group, POSCO, Gwangyang Works, South Korea*

Received 19 November 2006; received in revised form 2 July 2007; accepted 16 August 2007
Available online 22 October 2007

Abstract

Frozen meniscus features near the slab corners in continuous-cast ultra-low-carbon steel samples were investigated using special etching reagents and optical microscopy. The three-dimensional (3D) continuous shapes of hook defects along the oscillation marks around the slab corners were constructed from a set of micrographs taken at different vertical sections. The hook depth variation was traced around the slab perimeter. The maximum hook depth was observed at the corners and concave curvature was observed on a 45° vertical section from the corner. Horizontal cross-sections through the oscillation marks near the corners provide evidence that liquid steel overflow caused the oscillation mark. Shrinkage of the corner allows the overflowing steel to penetrate deeper into the larger corner gaps, giving rise to oscillation marks that point down in the casting direction at the corner. These results also explain the complex, 3D subsurface microstructures observed near the corners of the slab and quantify the hook depth and shape.

Keywords: Casting; Solidification microstructure; Ultra-low-carbon steel; Continuous casting

1. Introduction

Deep oscillation marks (OMs) [1] and subsurface hooks [2] in continuous-cast steel slabs are associated with many slab quality problems. Specifically, they tend to entrap argon bubbles and alumina inclusions near the hooks [3,4], leading to slivers and blisters, and transverse cracks often form near the roots of deep OMs [5–7]. In extreme cases, the entire slab surface must be ground or ‘‘scarfed’’ to remove all traces of the hook microstructure, resulting in high cost and loss of productivity [8]. As shown in Figs. 1 and 2, OMs are periodic depressions or grooves in the strand surface that run around the perimeter of continuous-cast steel. Subsurface hooks are distinctive microstructural features which extend from some oscillation marks and can be identified by etching transverse sections near the slab surface [1,2,6]. The curved hook in Fig. 1a contains a trapped argon bubble.

Hooks and OMs form due to many interdependent, transient phenomena that occur simultaneously during initial solidification near the meniscus. Several different mechanisms have been proposed in previous literature. Sengupta et al. [9] have recently suggested a new mechanism for hook and OM formation, that is illustrated in Fig. 1b. Hook formation starts when undercooled liquid steel at the meniscus freezes. Overflow of the solidified meniscus then occurs when the new liquid meniscus becomes unstable, which usually happens at the beginning of the negative strip period [10] during mold oscillation. Dendrites solidify away from the meniscus, which persists in the final microstructure as a distinct ‘‘line of hook origin’’. The extent to which

* Corresponding author. Tel.: +1 217 333 6919; fax: +1 217 244 6534.
E-mail address: bgthomas@uiuc.edu (B.G. Thomas).

1359-6454/$30.00
doi:10.1016/j.actamat.2007.08.035

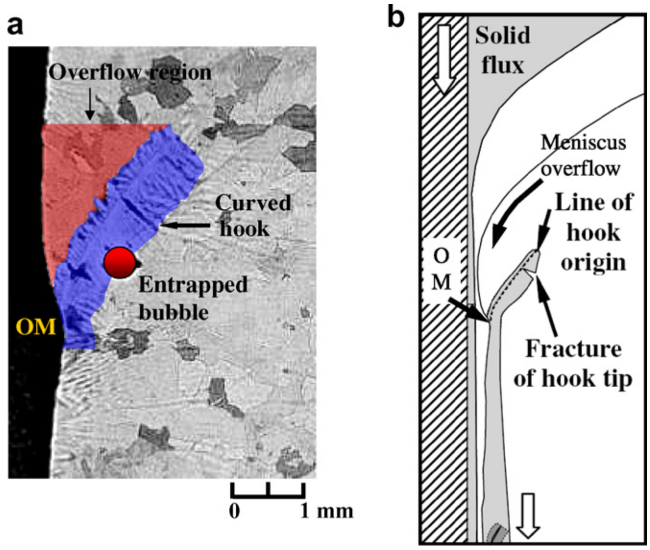

Fig. 1. Optical micrograph(a) of an ultralow-carbon steel sample showing entrapment of argon bubble by a curved hook-type oscillation mark and (b) schematic illustrating formation of curved hooks by meniscus solidification and subsequent liquid steel overflow [10].

the overflowing liquid steel can penetrate into the flux channel determines the final shape of the upper side of the OM.

This mechanism was proposed based on a careful analysis of numerous specially etched samples from ultra-low-carbon steel slabs combined with literature review, previous measurements, observation and theoretical modeling results [10]. It is supported by microstructural evidence obtained using [9] optical microscopy, scanning electron microscopy (SEM), electron backscattering diffraction (EBSD), energy dispersive X-ray spectroscopy (EDXS) and electron probe micro-analysis (EPMA) techniques. The truncated shape of the curved hook in Fig. 1a is explained by brittle fracture (hot tearing) of the fragile semi-solid near hook tip during overflow [10]. The fractured hook tip usually melts or is transported away by the flowing liquid steel, but a few micrographs contained a fractured hook tip that was captured nearby, proving this mechanism [9]. The slight microsegregation accompanying dendritic solidification showed that growth proceeded in both directions from the line of hook origin [9]. The line of hook origin was found to divide regions of different orientation in the steel, even after several phase transformations [9].

Previous understanding of hook and OM formation is based entirely on two-dimensional (2D) vertical-section micrographs, such as Fig. 1a, which reasonably represent the microstructure around most of the slab perimeter. Near the corners of the slab, however, OMs and hooks exhibit complex three-dimensional (3D) shapes, with different internal microstructures that were unknown before this work.

The present study was conducted to reveal the complex 3D shapes of the frozen meniscus hooks and OMs near the slab corners. Samples of ultra-low-carbon steel were studied because these grades ($C \leqslant 0.05\%$) are particularly prone to both OM and hook defects. A variety of cross-sections near the slab corners were specially etched and analyzed to distinguish the frozen meniscus shape, including vertical, horizontal and angle sections at different depths and locations in three slab samples taken from the slab corners. The results provide unique evidence of subsurface microstructural evolution in the meniscus region near the slab corners of continuous-cast steel.

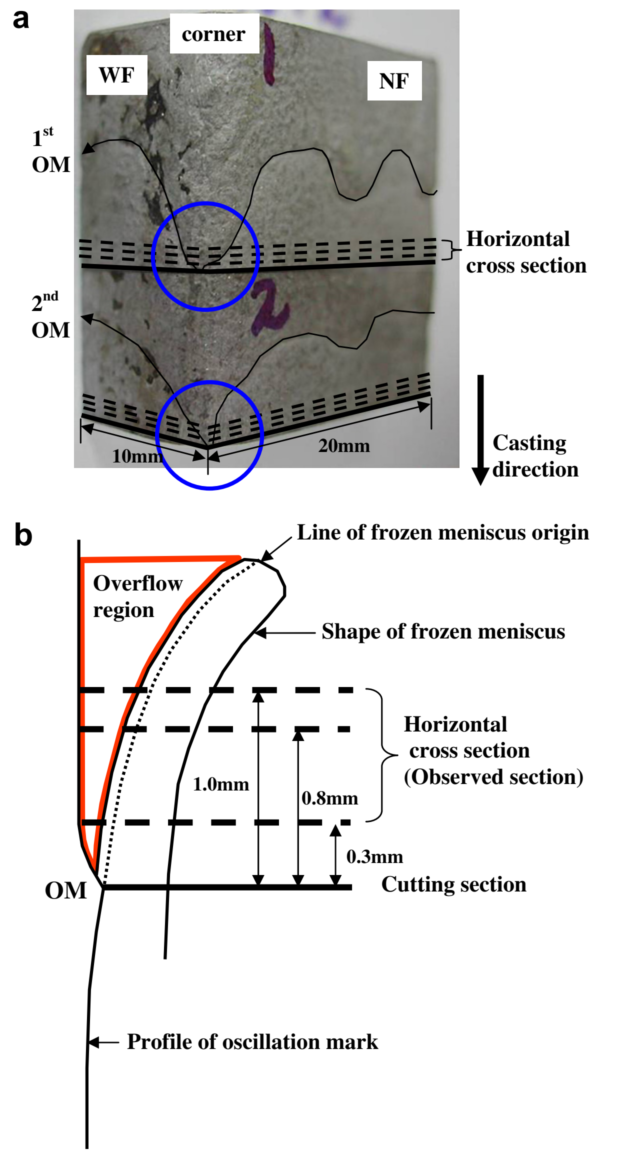

Fig. 2. Sample I (a) location obtained from slab corner and (b) three different horizontal sections cut for microscopy analysis of hooks and oscillation mark shown in circles.

2. Experimental

Samples from the slab corners of 230 × 1300 mm ultra-low-carbon steel slabs were obtained from plant experiments performed on the No. 2–1 conventional slab caster

Table 1
Casting conditions for slab samples

Sample number	Casting speed (m/min)	Slab width (mm)	Pour temperature (°Q)	Mold oscillation stroke (mm)	Mold oscillation frequency (cpm)	Non-sinusoidal mold oscillation ratio (%)	Superheat (°Q)	Electro-magnetic current (A)
Sample I	1.45	1300	1559	7	145	12	26	300
Sample II			1571	5	174	12	38	300
Sample III			1559	7	124	0	26	300
Heat 4	1.47	1570	1571	6.9	159	12	38	277
Heat 5			1567	6.9	160	12	34	0

Note: Samples I, II and III are from tests 3, 9 and 10, in Ref. [11]. Heat 4 and 5 are from Ref. [8].

at POSCO, Gwangyang Works, South Korea, which features a conventional parallel-mold, standard two-port submerged entry nozzle, non-sinusoidal hydraulic mold oscillator and electromagnetic brake ruler system. The casting speed was kept relatively constant at 1.45 m min^{-1}. Table 1 summarizes the casting conditions employed during casting of the slabs that contained the samples. The casting conditions of samples I, II and III matched the conditions of Tests 10, 3 and 9 in Ref. [11], respectively. Further details of these plant experiments, including the composition of the ultra-low-carbon steel grade and mold powder are given in Ref. [11].

Sample I (10 mm wide × 20 mm deep × 20 mm long) encompassed two OMs and was obtained near the corner, as shown in Fig. 2a. Horizontal sections were cut through the tip of the oscillation marks at the corner at 0.3, 0.8 and 1.0 mm locations above the OM tip, as shown in Fig. 2b. Optical micrographs are presented for the first oscillation mark.

Sample II (13 mm wide × 20 mm deep × 30 mm long) encompassed four OMs and was obtained near the corner of a different slab, as shown in Fig. 3a. Vertical sections through this sample were taken at various distances (0.7 to ~5.5 mm) from the wide face surface, by polishing, etching, photographing and then regrinding at intervals of ~0.5 mm, as shown in Fig. 3b. These sections parallel to the wide face revealed characteristic subsurface microstructural features, which were interpreted by extracting hook shapes to construct the 3D hook shape. Further vertical sections were taken at 20, 75 and 115 mm (center line) from the slab corner from the same slab, and hook depths and shapes were measured from micrographs of each section.

Sample III (100 mm long and encompassing nine OMs) was obtained near the corner from a different slab and was divided into three pieces each ~30 mm long, as shown in Fig. 4a. Each sample was then cut at a different vertical orientation to reveal the subsurface microstructures, as shown in Fig. 4b–d.

Further slab samples were taken for other conditions (Heats 4 and 5 [8]) and hook depths were measured from vertical sections taken from each sample around the perimeter of the narrow face (five locations) and wide face (seven locations).

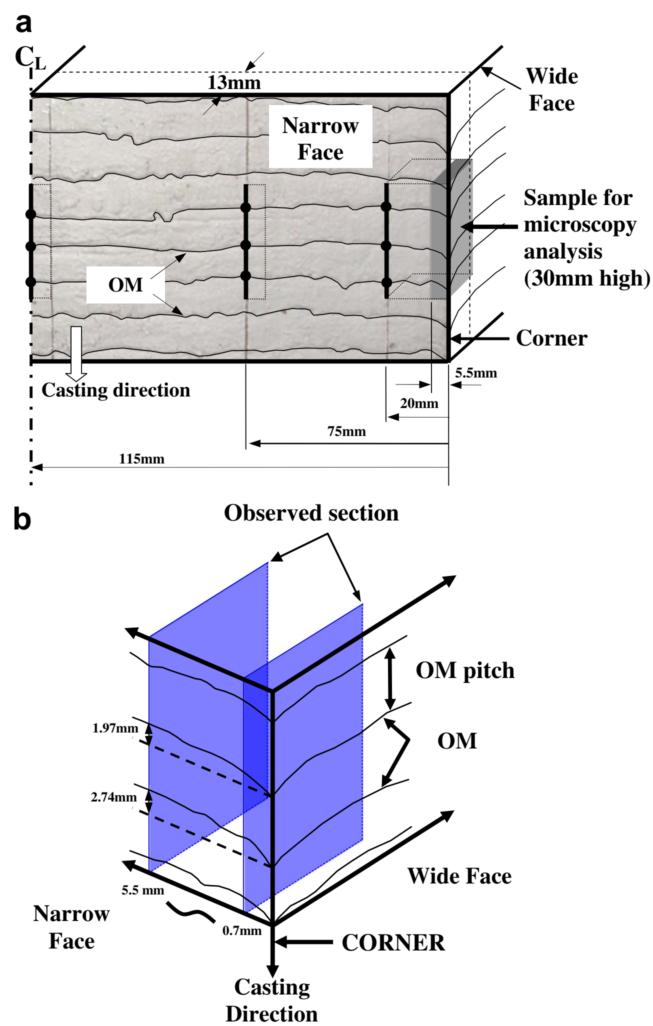

Fig. 3. Sample II (a) location obtained from slab corners and (b) location of sections cut for microscopy analysis showing oscillation mark shape.

All of the sections were ground, polished and then etched by a special etching method [10] to reveal the microstructure and hook shapes in ultra-low-carbon steel samples. The etching reagent was picric acid solution (2,4,6-trinitrophenol) with additions of the surfactant zephiramine (benzyldimethyl-*n*-tetradecylammonium chloride)

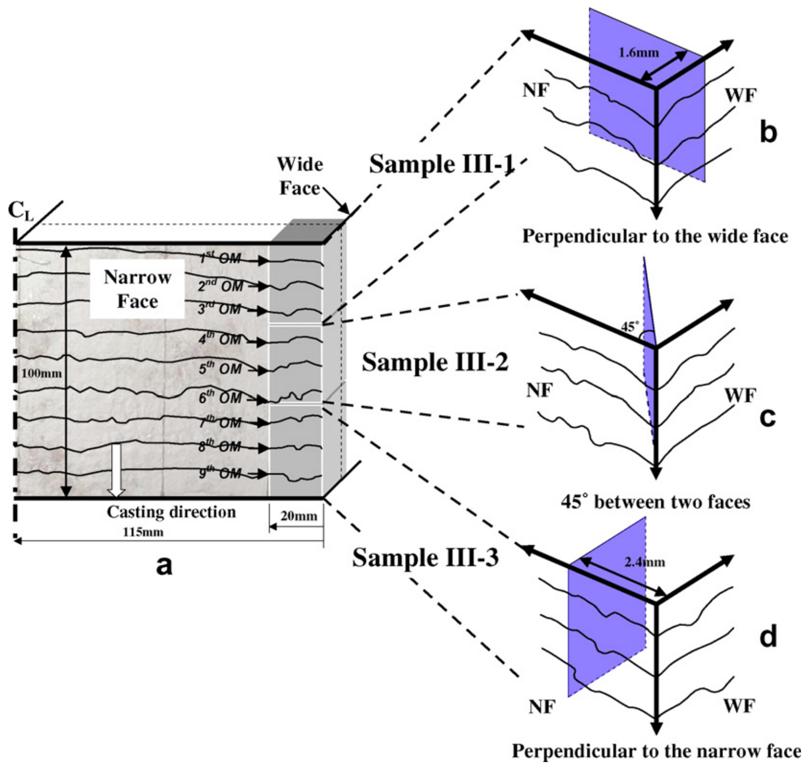

Fig. 4. Sample III (a) location obtained from slab corners and (b–d) orientation of three different vertical sections cut for microscopy analysis.

and etched for ∼1–1.5 h. Further details are given elsewhere [10].

3. Results and discussion

3.1. Overflow mechanism of liquid steel at the corner

Oscillation marks are well-known to "point" downwards at the corners, indicating the casting direction, as in Fig. 2a. The lowest point of each oscillation mark is found at the corner, extending 2–3 mm below the average around the perimeter, as shown in Fig. 3b. The reason for this is clarified by analysis of the horizontal section micrographs of sample I in Figs. 2 and 5, which also reveals new insights into hook formation in the slab corner.

Each micrograph in Fig. 5 exhibits two distinct layers of frozen steel at the corner, which formed at different times. The schematic in Fig. 2b, explains the appearance of these microstructural features. After the 3D meniscus in the corner freezes to form the hook, it shrinks to pull away from the mold walls. Liquid steel overflows the solidified meniscus – as pictured in Fig. 1b – and then flows down into the corner gap between the hook and the mold. It can flow further downward in the corner region, owing to the shrinkage gap there. As the overflowing liquid freezes, its horizontal cross-section naturally decreases, ultimately ending in a tip, which forms the point of the OM tip at the corner. A small thin layer, which is delineated by a solid red line in Fig. 5, is seen on the surface at the corner and clearly shows evidence of this phenomenon. The area outlined by this solid red line decreases in size with decreasing vertical distance to the OM point (i.e., from 1.0 to 0.8 to 0.3 mm). These areas slice through the base of the hook, which was originally the frozen meniscus. Furthermore, the enlarged inset in Fig. 5c clearly shows valleys on each side of this surface layer, which represent the vertical component of the steep-sloping OMs near the corners, observed in Fig. 2a. The distinct microstructure of this layer indicates that it formed later, from liquid running down the surface.

The tip of this overflowed region penetrates further into the corner, where the gap between the mold and the frozen meniscus hook is largest. This larger gap also decreases heat transfer in the corner prior to the overflow, leading to less meniscus freezing. This explains why the hook is thinner in the corner, which is seen by following the hook, demarked by the dark thin discontinuous subsurface line, around the corners in Fig. 5.

3.2. Analysis of 3D subsurface hook shape around the corner

Micrographs of vertical sections (sample II) presented in Fig. 6 show great differences in hook shapes near the corner. The curved line along the center of each hook represents the "line of origin" of the hook and indicates the shape of the meniscus when it froze. Solidification then proceeded in both directions away from this line, slowing temporarily when thermal gradients diminished, to leave the dark bands that outline each hook. The lines of hook origin traced from a series of 10 such vertical sections are

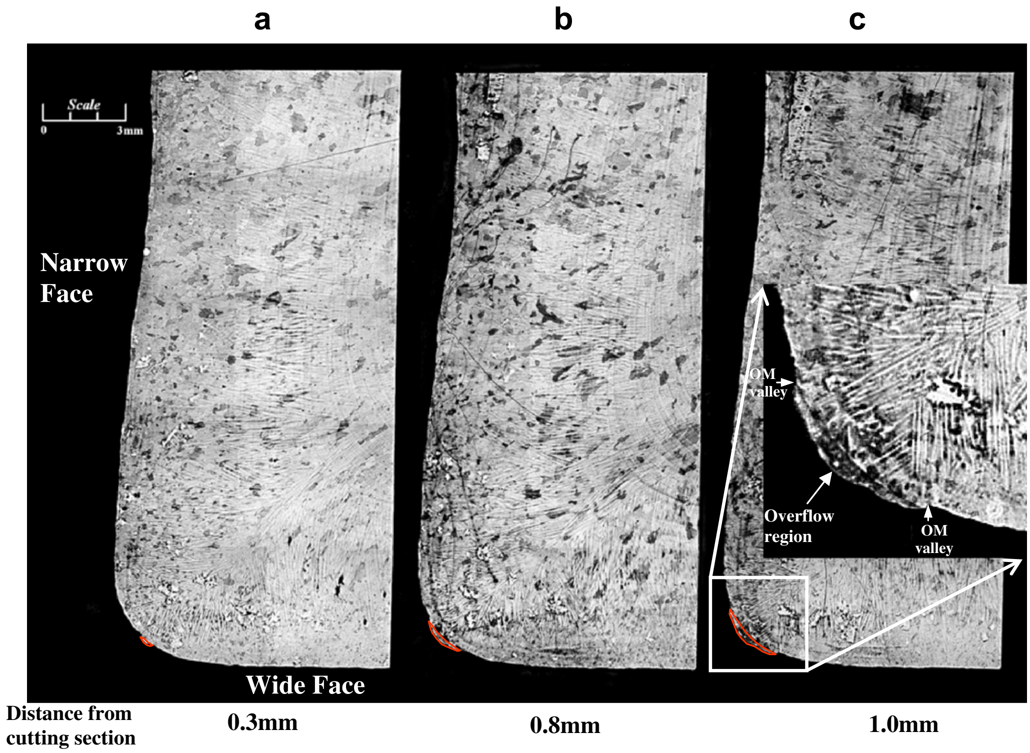

Fig. 5. Optical micrographs of horizontal cross sections (sample I) showing evidence of liquid steel overflow (outlined).

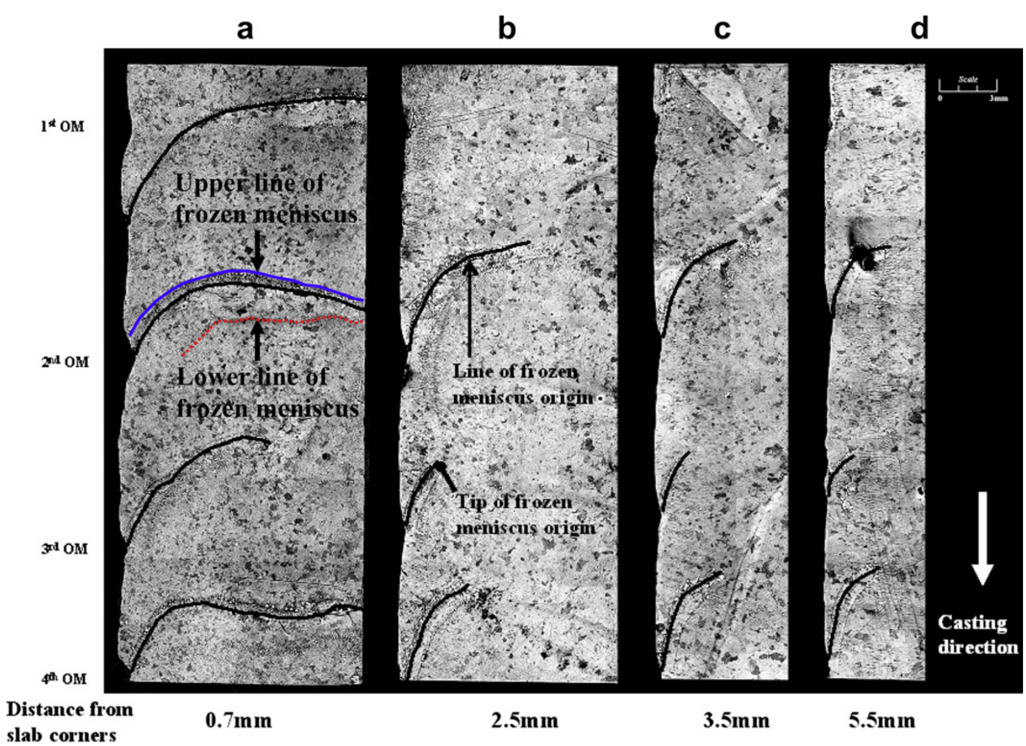

Fig. 6. Optical micrographs at different distances from wide face (sample II): line of frozen meniscus shows origin of "hook"; upper and lower lines show hook thickness.

shown in Fig. 7a. A true 3D schematic of the hook shape around the slab corner, given in Fig. 7b, was constructed from the hook outlines surrounding the second OM. The upper lines (solid) outline the liquid that overflowed the frozen meniscus. The lower lines (dashed) indicate the boundary between the supercooled frozen meniscus and the molten steel pool below. The vertical distance in Fig. 7 is measured in the casting direction relative to the

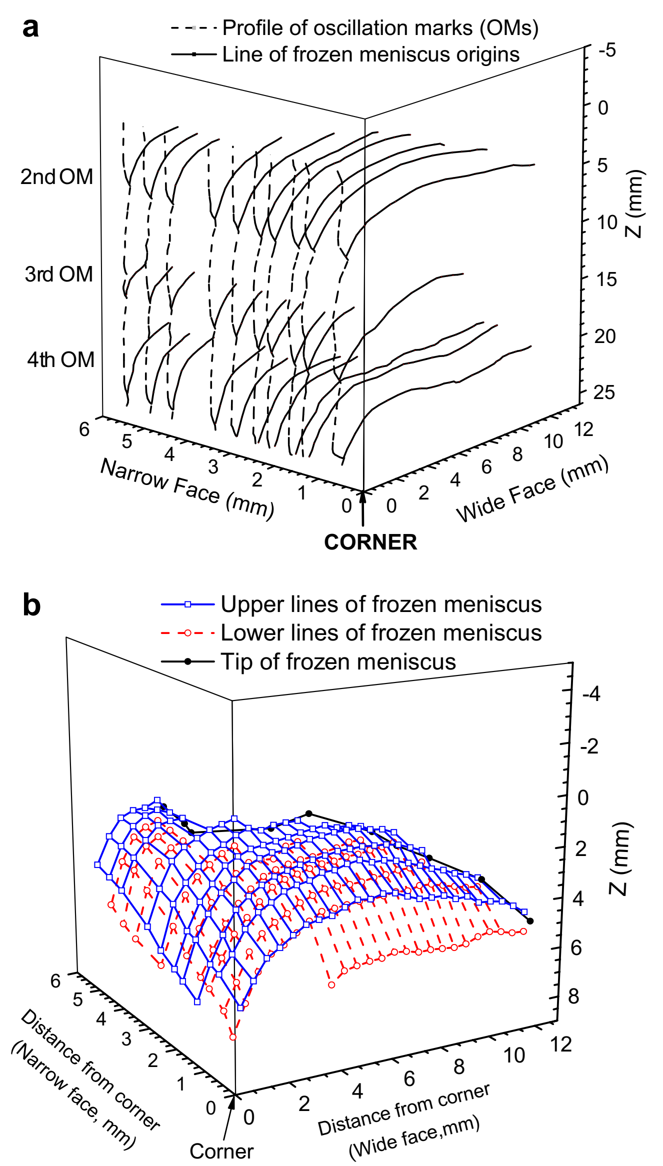

Fig. 7. Line of frozen meniscus origins obtained from micrograph analysis of sample II (a) and (b) 3D shape of frozen meniscus hook at 2nd OM.

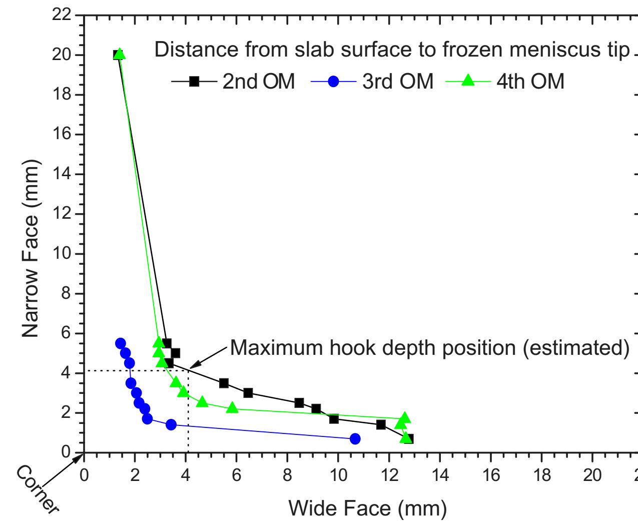

Fig. 8. Top views of lines of frozen meniscus origins (hooks) from micrographs (sample II) showing hook depth increase around corner and explanation of hook depth variations observed in micrographs.

arbitrary zero-reference height taken midway between the first and second oscillation marks.

Fig. 8 was constructed to show the top view of the three OM hooks in Fig. 7a. This graph clearly reveals the 3D shape of the frozen meniscus and hooks, which extends continuously from the OM perimeter around the slab corner. The third OM hook is consistently smaller than its neighbors. This indicates that changes in meniscus conditions extending around the corner but lasting less than a second are very common. This is likely due to transient fluid-flow phenomena, such as surface level and superheat fluctuations, which vary even under steady casting conditions. Fig. 8 also explains the observation in Fig. 6 that the second OM hook is triple the depth of the third OM at 2.5 mm from the corner, but only twice the depth at 3.5 mm.

The micrograph in Fig. 9a shows the deepest extent of the hooks, which is observed in a 45° vertical cross-section from the corner, as shown in Fig. 4c. Fig. 9b shows the approximate 2D hook shape constructed at different vertical sections through different oscillation marks near the corner. The hooks at the corner start ~0.75 mm lower than other two nearby observations. This indicates the downward-pointing OM caused by the furthest penetration of overflowing liquid steel into the flux channel at the corners, as discussed earlier. Narrow-face hooks are slightly deeper than wide-face hooks, owing to the generally lower superheat there, and correspondingly more meniscus freezing. This effect is greatly exaggerated in Fig. 9b, due to the proximity of the 2D sections to the corner. This same reason causes the difference between hook depths in Fig. 6, and is explained with Fig. 8.

Fig. 9b also shows that corner hooks at the 45° plane sometimes exhibit concave curvature. At other locations, hooks are always convex-shaped and match well with Bikerman's equation, as observed clearly in previous work [8–11]. This concave curvature at the corner can not predicted by the 2D equilibrium meniscus shape of Bikerman's equation, which is determined solely by the balance of surface tension and ferrostatic pressure forces [12,13]. This observation suggests that other effects, such as 3D, transient pressure variations caused by the moving slag rim attached to the mold wall, are more influential near the slab corners than elsewhere. This is consistent with a thicker solidified flux rim in the colder corners.

3.3. Hook shape around slab perimeter

Fig. 10 compares hook depths around the perimeter of slab sample II, as shown in Fig. 3a. The maximum hook depth appears at the corners, owing to further meniscus

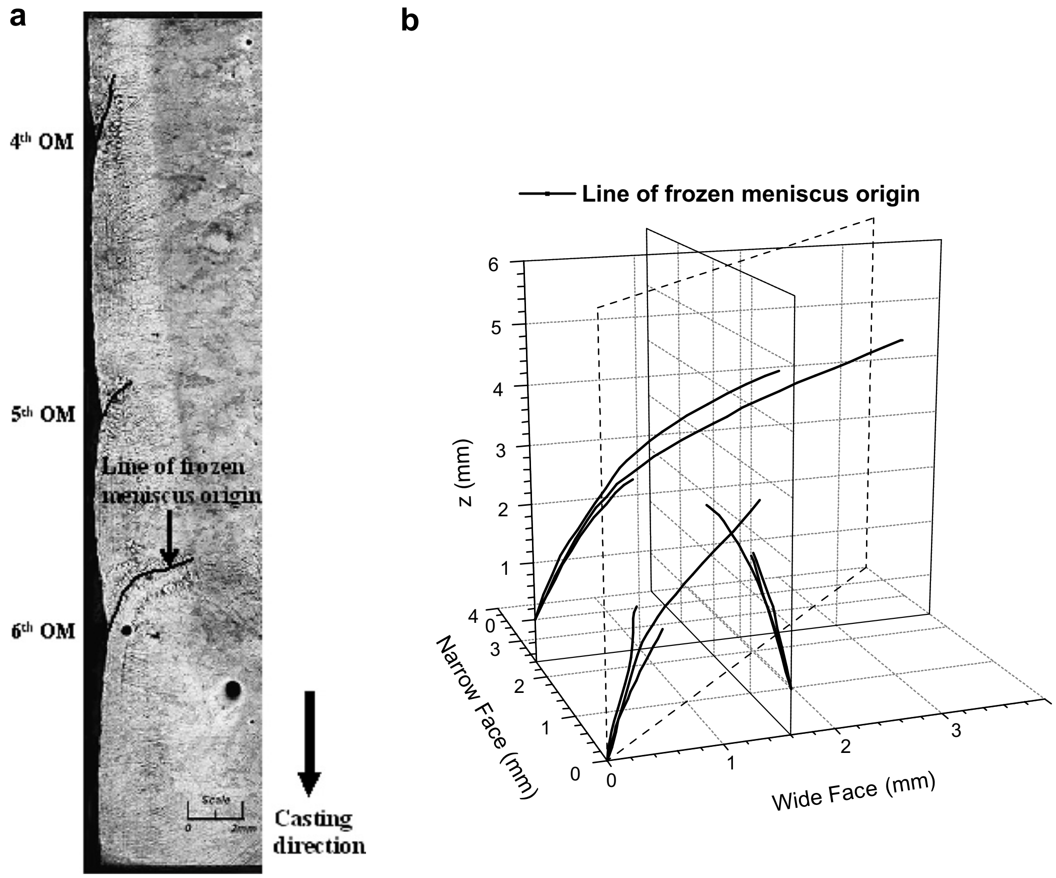

Fig. 9. Hook shapes (lines of frozen meniscus from vertical sections through sample III) (a) micrograph of 45° section and (b) shapes traced from three different hooks.

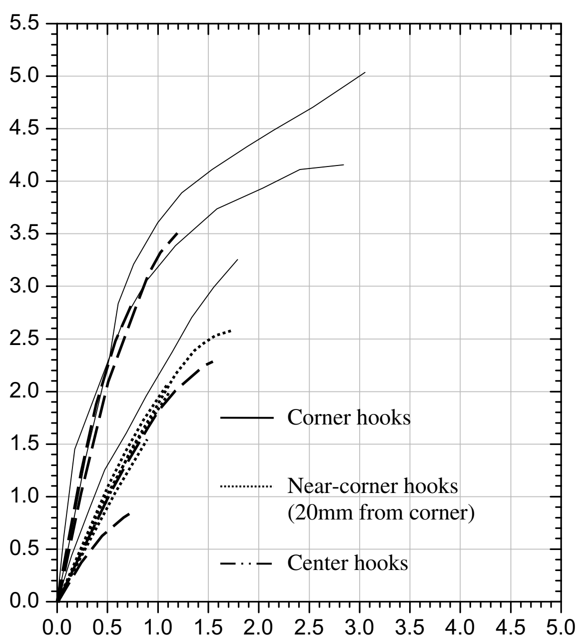

Fig. 10. Lines of frozen meniscus (sample II) at three locations around slab perimeter of narrow face, showing increase in hook size towards corner.

solidification, likely due to the colder liquid found in this region. Hook depths [8] measured around the slab perimeter are shown in Fig. 11. Hooks extend continuously around the entire slab perimeter, although they are often difficult to etch. The hooks are usually deepest at the corners, by 10–100%. Differences between the inner- and outer-radius wide faces (front and back sides) of the strand are negligible relative to the local variations. Hooks are often deeper towards the narrow faces although significant asymmetry is observed between sides.

4. Conclusions

The 3D shape of the frozen meniscus, subsurface hook microstructure and oscillation marks in continuous-cast ultra-low-carbon steel slabs has been investigated by analyzing micrographs of carefully etched samples near the corners. The horizontal sections provide clear evidence that OM formation is due to liquid steel overflow. The line of hook origin in the subsurface microstructure indicates the original shape of the frozen meniscus.

A graphical reconstruction of the 3D hook shape in the corner from a series of vertical cross-sections explains the

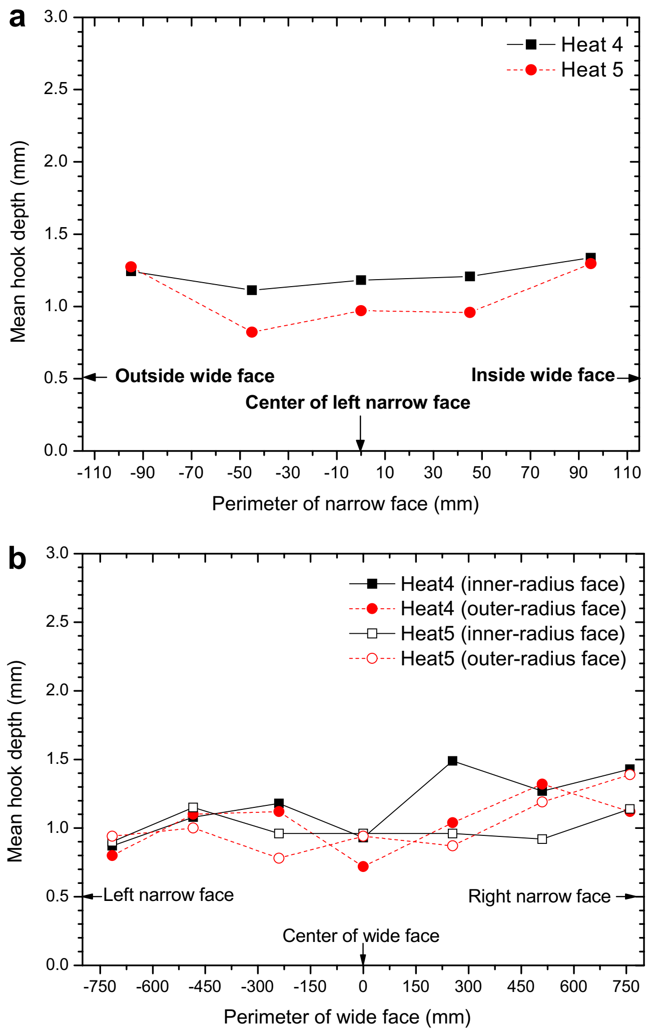

Fig. 11. Hook depth variation along mold perimeter of (a) narrow face and (b) wide face.

progression of 2D hook microstructures observed around the slab perimeter. The classic 2D hook microstructure simply curves continuously around the corner, increasing in size towards the corner. The shape, size and depth of this continuous hook structure have been quantified.

The 3D shape of the continuous plane of hook origin matches the expected shape of the frozen meniscus in the corner. Deeper hooks in this region might arise from lower superheat, or higher pressure from the deeper flux rim during mold oscillation expected in the corner. These results confirm the mechanism for the formation of hooks and OMs by meniscus solidification and subsequent liquid steel overflow suggested by Sengupta et al. [9]. Oscillation marks extend further in the casting direction at the corner due to the ease of liquid steel overflow into the larger gap there. These results will provide a foundation for future computational models and plant trials to understand and control hook and OM formation near the slab corners.

Acknowledgements

Financial support from the Korea Research Foundation Grant funded by the Korean Government (MOEHRD), (KRF-2005-213-D00110), the Continuous Casting Consortium at the University of Illinois at Urban-Champaign and the National Science Foundation (Grant DMI 04-23794) is acknowledged for support this project. The authors also thank Dr. J. Sengupta for providing initial help and POSCO, Gwangyang Works, S. Korea for providing the samples.

References

[1] Takeuchi E, Brimacombe JK. The formation of oscillation marks in the continuous casting of steel slabs. Met Trans B 1984;15B:493–509.
[2] Emi T, Nakato H, Iida Y, Emoto K, Tachibana R, Imai T, et al. Influence of physical and chemical properties of mold powders on the solidification and occurrence of surface defects of strand cast slabs. Proc Nat Open Hearth Basic Oxygen Steel Conf 1978;61:350–61.
[3] Schmidt KD, Friedel F, Imlau K, Jager W, Muller KT. Consequent improvement of surface quality by systematic analysis of slabs. Steel Res Int 2003;74(11–12):659–66.
[4] Birat J, Larrecq M, Lamant J, Petegnief J. The continuous casting mold: a basic tool for surface quality and strand productivity. In: Cramb AW, Szekeres E, editors. Mold operation for quality and productivity. Iron and Steel Society. Warrendale, PA; 1991. p. 3–14.
[5] Brimacombe JK, Sorimachi K. Crack formation in the continuous casting of steel. Metall Trans B 1977;8B:489–505.
[6] Takeuchi E, Brimacombe JK. Effect of oscillation-mark formation on the surface quality of continuously cast steel slabs. Met Trans B 1985;16B:605–25.
[7] Harada S, Tanaka S, Misumi H, Mizoguchi S, Horiguchi J. A formation mechanism of transverse cracks on CC slab surface. ISIJ Int 1990;30(4):310–6.
[8] Shin H-J, Thomas BG, Lee GG, Park JM, Lee CH, Kim SH. Analysis of hook formation mechanism in ultra low carbon steel using CON1D heat flow – solidification model. Materials science & technology. New Orleans, LA: TMS, Warrendale, PA; 2004. II. p. 11–26.
[9] Sengupta J, Shin H-J, Thomas BG, Kim S-H. Micrograph evidence of meniscus solidification and sub-surface microstructure evolution in continuous-cast ultra-low carbon steels. Acta Mater 2006;54(4):1165–73.
[10] Sengupta J, Thomas BG, Shin HJ, Lee GG, Kim SH. Mechanism of hook formation during continuous casting of ultra-low carbon steel slabs. Metall Mater Trans A 2006;37A(5):1597–611.
[11] Shin H-J, Lee GG, Choi WY, Kang SM, Park JH, Kim SH, et al. Effect of mold oscillation on powder consumption and hook formation in ultra low carbon steel slabs. AISTech. Nashville, TN: Assoc. Iron Steel Technology; 2004.
[12] Bikerman JJ. Physical surfaces. New York: Academic Press; 1970.
[13] Fredriksson H, Elfsberg J. Thoughts about the initial solidification process during continuous casting of steel. Scand J Metal 2002;31:292–7.